

Lars Hahn*,
Steffen Rittner,
Dominik Nuss,
Moniruddoza Ashir,
Chokri Cherif

Development of Methods to Improve the Mechanical Performance of Coated Grid-Like Non-Crimp Fabrics for Construction Applications

DOI: 10.5604/01.3001.0012.7508

Technische Universität Dresden,
Faculty of Mechanical Science and Engineering,
Institute of Textile Machinery
and High Performance Material Technology,
Dresden, Germany
* e-mail: lars.hahn@tu-dresden.de

Abstract

This paper presents investigations aiming to improve the impregnation of a coating agent and thus increase the mechanical performance of geogrids, especially grid-like non-crimp fabrics (NCF) consisting of carbon fiber heavy tows (CFHT). The squeezing process is industry standard, but the relationship between the machine setting parameters (squeezing pressure and hardness of squeeze roll surface) and the impact on the tensile strength of grid-like NCF is still unexplored. The setting parameters evaluated lead to an increase in tensile strength of up to 10% compared to grid-like NCF coated without the squeezing process. Additionally the first insights into the coating process supported by ultrasonic vibrations based on CFHT single yarns are provided. It is shown that the tensile strength of treated CFHT can be increased by up to 12%, in comparison to CFHT coated without ultrasonic vibrations.

Key words: carbon fiber heavy tows, impregnation, coating, textile reinforced concrete, non-crimp fabric.

Introduction

Textile-reinforced constructions from glass or carbon yarns have a high load capacity and offer great potential for new architectural applications due to the flexibility and lightweight of the reinforcement structure [1-7]. For the production of textile reinforcements, so-called grid-like non-crimp fabrics (NCF), the multiaxial warp knitting process is an established manufacturing technology [6, 8-11]. Since these textile reinforcements do not have to be protected against corrosion, they enable thin-walled constructions. Thus this material is an excellent option for enormous savings in concrete.

The load-bearing capacity of textile reinforcements is significantly affected by

their coating [7, 12-14]. The functions of a coating agent are as follows: a). increase adhesion between concrete and fibers (external bond), b). ensure force transmission between internal filaments (internal bond), c). strengthen the geometry of the structure for the concreting process, and d). protect the fibers against environmental influences [6, 9, 14-16]. Furthermore the complete penetration of the coating agent over the yarn cross-section is of great importance for high utilization of the load-bearing capacity of textile reinforcements [6, 9]. If the coating does not penetrate the entire yarn cross-section (outer and inner filaments), the mechanical performance of the yarn is insufficiently exploited, because the forces applied are not transmitted to the inner filaments, see *Figure 1*.

The force acting on the construction is transmitted from the concrete matrices to the outside filaments of the yarn. However, the force cannot be transmitted to the core of the yarn if the inner filaments are uncoated [6]. In this case, force transmission between filaments takes place exclusively by friction [7]. Krüger et. al. and

Lorenz described by means of pull-out tests how the coating (styrene butadiene dispersion and epoxy resin) influences the force transmission from the core of the yarn to the inner filaments [12, 17]. Also Shilang et. al. illustrated the effect of an increase in frictional bond strength by coating the reinforcement yarns with a coating agent (epoxy) [8]. With epoxy-based impregnations, textile reinforcements typically result in stiff structures e). grid-like NCF plates. For the research described here, styrene butadiene dispersion (SBR) coating was used to ensure the flexibility of the reinforcement structures manufactured.

In addition, the investigations of Köckritz showed that the coating (SBR) of the textile reinforcement fibers improved the bonding between the concrete matrix and filaments in terms of glass fibers [11]. The behaviour is caused by the Poisson ratio effect and bundling effect, which led to increased friction between the inner filaments. Moreover investigations carried out by Kulas introduced SBR as a potential coating for carbon reinforcements [7].

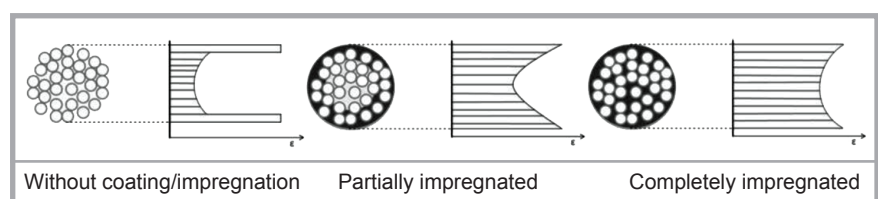


Figure 1. Coating-dependent stress distribution in multifilament yarn [1].

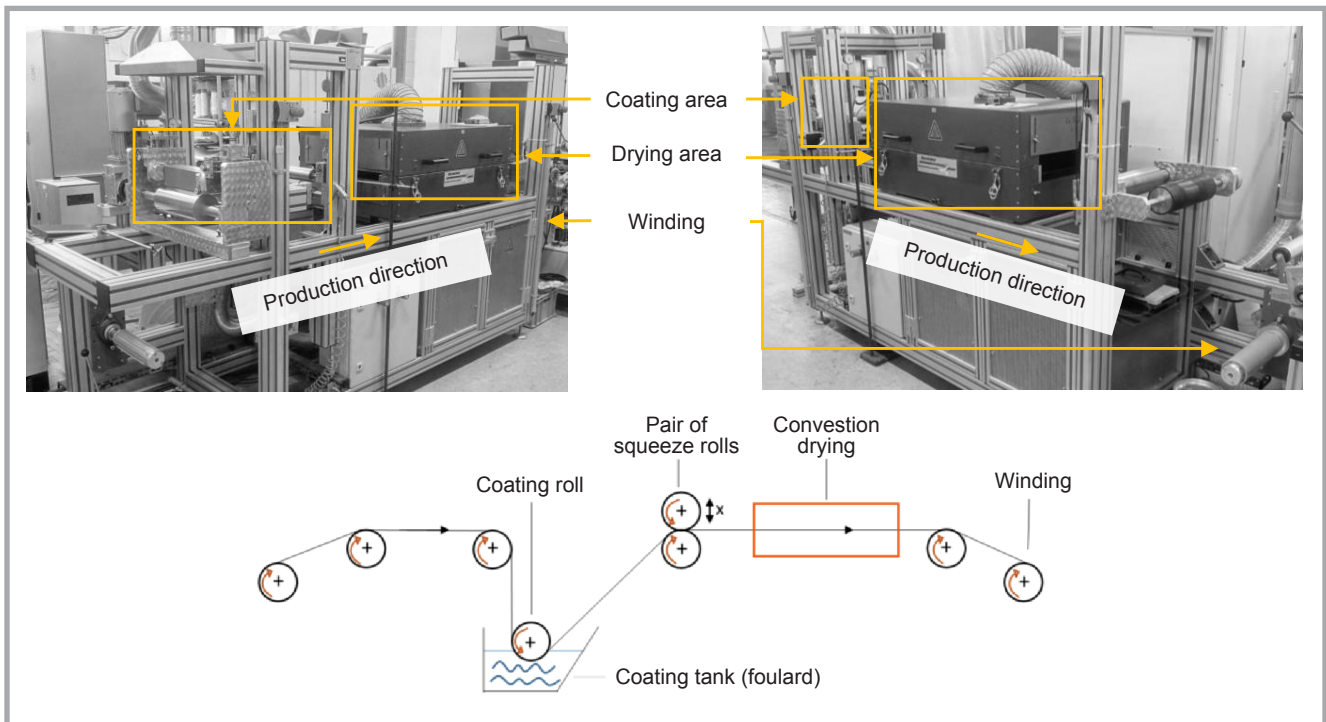


Figure 2. Coating machinery (Basecoater COATEMA Coating Machinery GmbH BC32).

As shown, the fundamental effects of the coating composition on the mechanical stability of the textile reinforcement have been extensively researched. However, the relationship between the preferential machine configuration for the coating process and the impregnation behaviour as well as the resulting tensile strength of the coated CF grid-like reinforcement structure have not yet been thoroughly studied. Thus initial experimental investigations were performed to define how selected machine parameters of the coating process influence the impregnation depth of high-performance textile grids consisting of CFHT. The focus during the research project was on the squeezing process as an integral part of the coating process. This

process is industry standard, however, the relationship between the machine setting parameters such as the squeeze pressure and hardness of the squeeze roll-surface and the impact on the tensile strength of the coating agent content of grid-like non-crimp fabrics consisting of CFHT is still unexplored. Additionally first insights into the coating process supported by ultrasonic vibrations based on CFHT single yarns are provided.

Experimental

The influence of selected machine setting parameters (see **Table 3**) on the tensile strength and impregnation of roving cross-sections was determined by tensile

tests and microscopic analyses. In addition, this paper provides a first insight into the excitation of the coating composition by ultrasonic vibration and its impact on the impregnation behaviour and tensile strength of coated CFHT.

Materials

As basic material for investigations on the squeezing process, grid-like non-crimp fabrics (NCF) made of carbon fiber heavy tows (CFHT), 48k in the 0° direction and 12k filaments in the 90° direction, were produced on a multiaxial warp knitting machine – Malitronic® of the Institute of Textile Machinery and High Performance Material Technology (ITM). The coating material selected comprised a watery dispersion based on styrene butadiene dispersion (SBR), which is termed Lefasol VL90/1, see **Table 1**. To solidify the coating agent, the harder Lefasol VP 4-5 LF was added.

Additional technical specifications of the textile materials used are displayed in **Table 2**.

The application of the coating agent to NCF was performed on a Basecoater COATEMA from Coating Machinery GmbH BC32, Germany (see **Figure 2**). For all experiments described within this paper, foulard coating was chosen as the basic coating method.

Table 1. Specifications of the coating materials used.

Coating material	Solid content, %	Linking temperature, °C	Mixing ratio, %
Lefasol VL90/1	50 ± 1	130-160	95.3
Lefasol VP 4-5 LF	75 ± 2	130-200	4.8

Table 2. Specifications of the textile materials used.

Fiber material, carbon fiber heavy tows (CFHT)	0° direction		90° direction
	Product name	Tenax® STS40 F13	Tenax® -E HTS40 F13
Number of filaments	48k	12k	
Linear density (Tt)	3200 tex	800 tex	
Sizing	1 % Polyurethane		
Grid-like non-crimp fabric (NCF)	Axial distance	14.3 (±2 mm)	10.7 (±2 mm)
	Width of textile rolls	300 mm	
	Area weight (uncoated)	374 g/m ²	

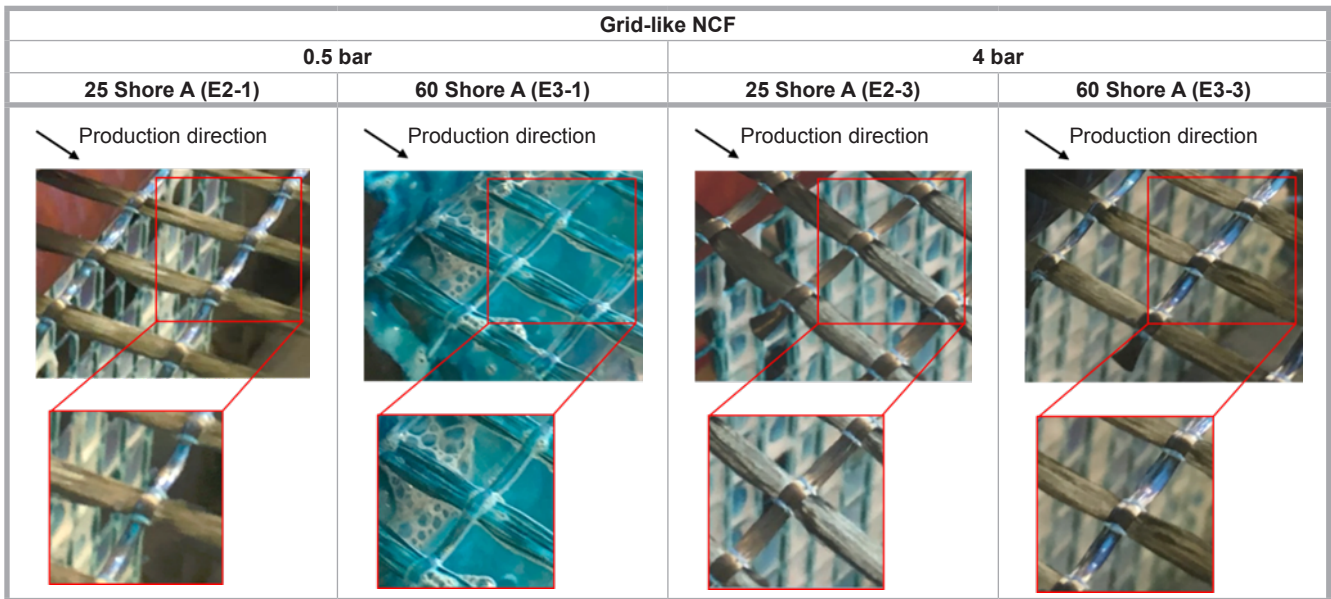


Figure 3. Exemplary representation of the coating behavior of grid-like NCF in dependent selected machine setting parameters (squeezing pressure and hardness of squeeze roll surface).

To determine the influence of the selected coating parameters on the quality of impregnation (penetration depth) and on the tensile strength of the textile materials, the experimental design presented in **Table 3** was used. The following series of experiments were carried out: varying the squeeze roll surface hardness, squeezing pressure and roll materials between rolls located above and below the grid-like NCF using *grid-like NCF*. Further experiments were done by excitation of the coating agent through ultrasonic vibration using *single yarn made of CFHT*, based

on the machine PALSSONIC PTIC-6-ES (Allpax GmbH & Co. KG, Germany) see **Figure 4**. For all experiments, a process speed of 0.3 m/min and oven temperature of 160 °C were used for drying and curing of the coating agent.

Methods

For characterisation and analysis of the selected coating parameters (see **Table 3**: hardness of squeeze roll surface upper/lower, squeezing pressure, and ultrasonic excitation of the coating agent), the following methods were applied.

Determination of the coating agent content: In order to determine the amount of coating agent applied, according to the standard DIN EN ISO 12127, dry samples were compared with the coated samples produced regarding their basis weight [18]. A precision balance was used to determine the coating agent content.

Microscopic analyses of the CFHT cross-section: In order to investigate the link between coating agent content and impregnation depth, micrographs of the CFHT cross-section were developed by means of microsection segments. The micrographs were recorded using a reflected-light microscope AXIOImager.M1m from Carl Zeiss AG (Germany), at 25x and 100x magnifications. In the section *Results and Discussion*, selected micrographs will be presented.

Characterisation of the mechanical tensile strength. As shown in **Figure 1**, the penetration depth of the coating agent

Table 3. Overview of samples.

Experiment number	Sample	Parameter			
		Hardness of squeeze roll surface, in Shore A		Squeezing pressure, in bar	Ultrasound, in kHz
		Upper	Lower		
Grid-like NCF					
Reference (uncoated)	R1	–	–	–	–
Reference (coated)	R2	–	–	–	–
1	E1-1	25	25	2	–
	E1-2	50	50		
	E1-3	60	60		
2	E2-1	25	25	0.5	–
	E2-2			2	
	E2-3			4	
3	E3-1	60	60	0.5	–
	E3-2			2	
	E3-3			4	
4	E4-1	25	Steel	2	–
	E4-2			4	
Single yarn made of CFHT					
5	E5-1	60	60	4	–
	E5-2	60	60	4	25
	E5-3	60	60	4	45

Table 4. Pre-adjustments for the tensile strength testing method.

Sample holder	SPH 8270 /Vulkollan corrugated 60 x 50
Force tensor	10 kN
Position encoder	Optical elongation
Pre-force	0.5 cN/tex
Velocity of E-module	200 mm/min
Velocity of testing	200 mm/min
Clamping length	500 mm

Table 5. Schematics for the deformation behaviour of the squeeze rolls and grid-like NCF depending on roll surface hardness.

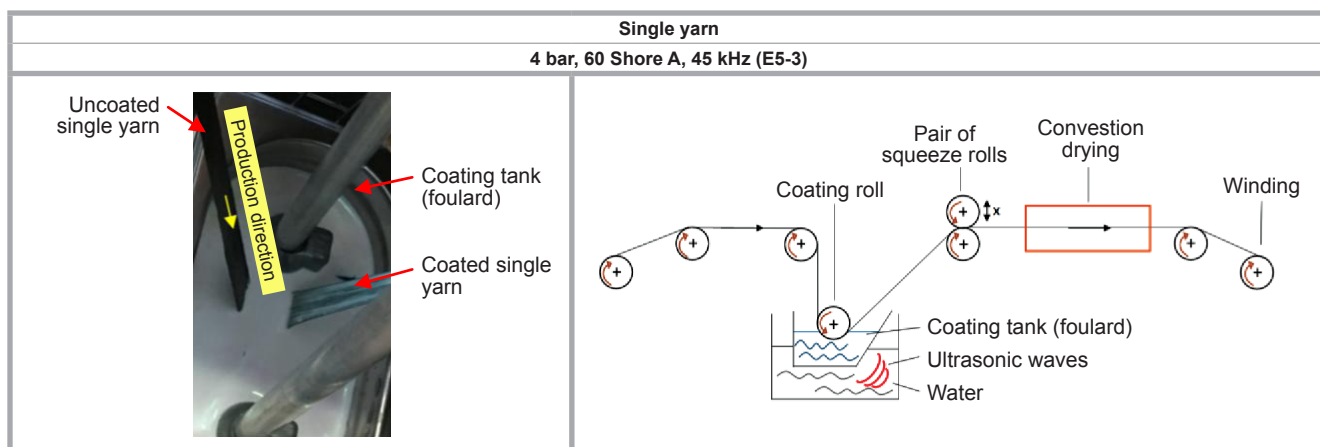
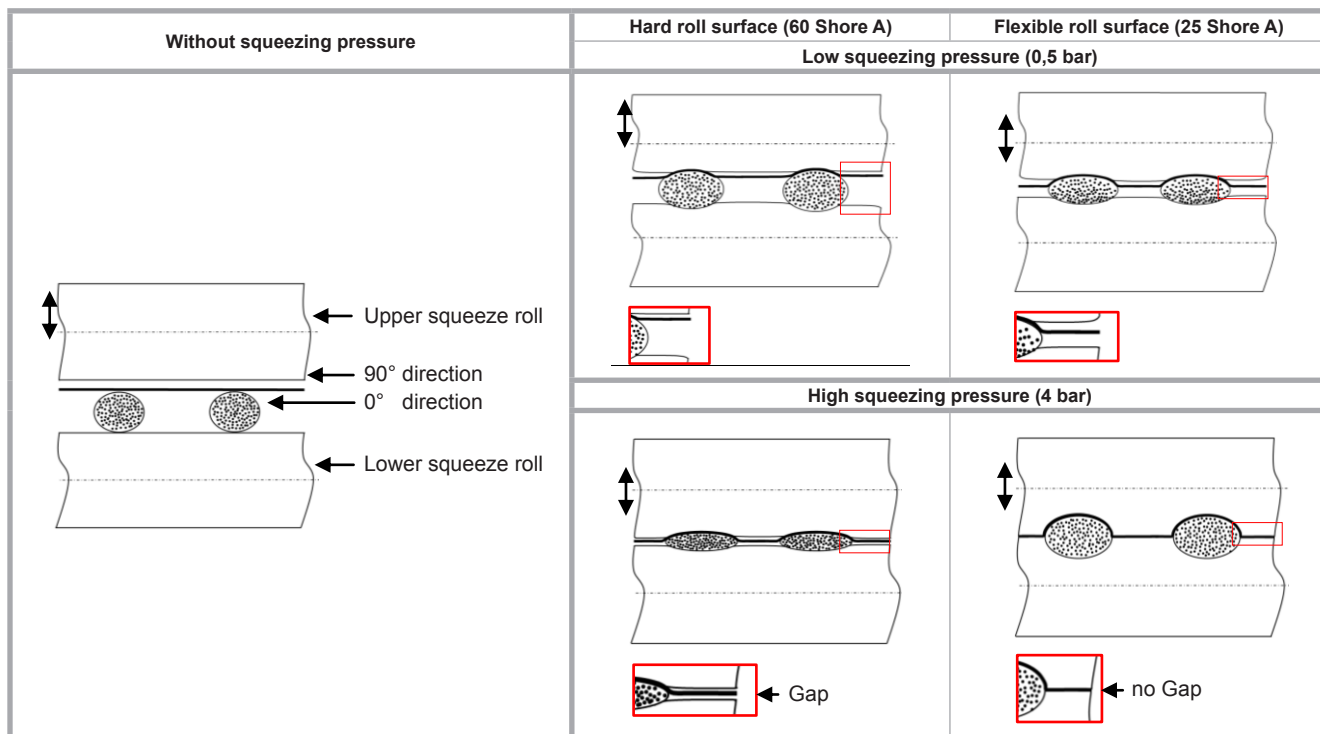


Figure 4. Exemplary representation of the coating behavior of single yarn.

significantly impacted the tensile strength of the carbon fiber. For this purpose, the tensile strength of coated samples was analysed to investigate how the selected coating parameters influence the mechanical behaviour of the grid-like NCF or single yarns. In the case of grid-like NCF samples, 0° yarns for characterisation of the tensile strength were excised in a defined manner. The tensile strength characterisations were based on DIN EN ISO 3341, and the length of the samples tested was approximately 1.2 m [19]. The tensile testing machine used was a ZWICK Z 100 (Zwick GmbH & Co. KG, Germany). Pre-adjustments for the tensile strength testing method are shown in **Table 4**.

Results and discussion

Analyses during sample preparation

Figure 3 shows an example of part of the coating experiments carried out. The coating tests indicate that the amount of the coating agent squeezed out of the grid-like NCF decreases with an increase in the hardness of the squeeze roll surface. In addition, it is noted that with the increasing surface hardness of the squeeze roll surface, blistering within the squeezed coating agent increases. Furthermore it is shown that the appearance of samples E2-1 (0.5 bar, 25 Shore A) and E3-3 (4 bar, 60 Shore A) looks similar. It means that the effect of the squeezing pressure and hardness of the squeeze

roll surface on the coating quality depend on each other. Consequently the squeezing process should be optimised depending on the hardness roll and squeezing pressure used. In addition, **Figure 3** shows that 0° yarns as well as 90° yarns of sample category E2-3 (4 bar, 25 Shore A) are squeezed. In the case of E2-1 and E3-3 (4 bar, 60 Shore A), only 0° yarns are squeezed, and coating agent residues are visible on the surface of 90° yarns. In conclusion, the 0° filaments of the E3-3 test series are effectively subjected to a higher pressure than the 0° filaments of the E2-1/3 test series, set at the coating unit (see **Figure 3** and **Table 5**). However, a statement about the impregnation of 0° rovings can only be made from further

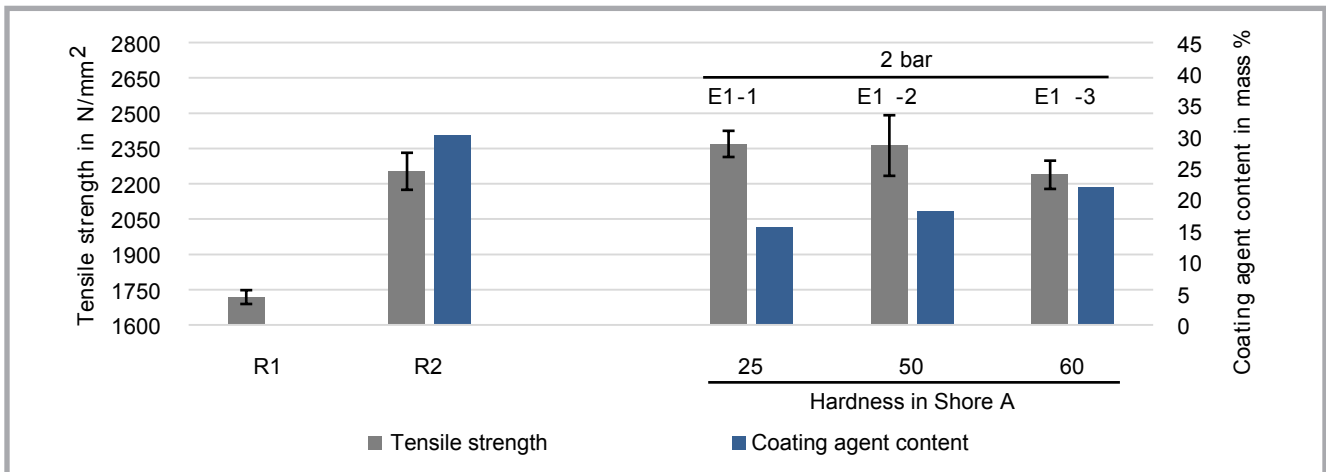


Figure 5. Increasing the hardness of the squeeze roll surface at constant 2 bar squeeze pressure (R1: Reference uncoated, R2: Reference coated without squeezing process).

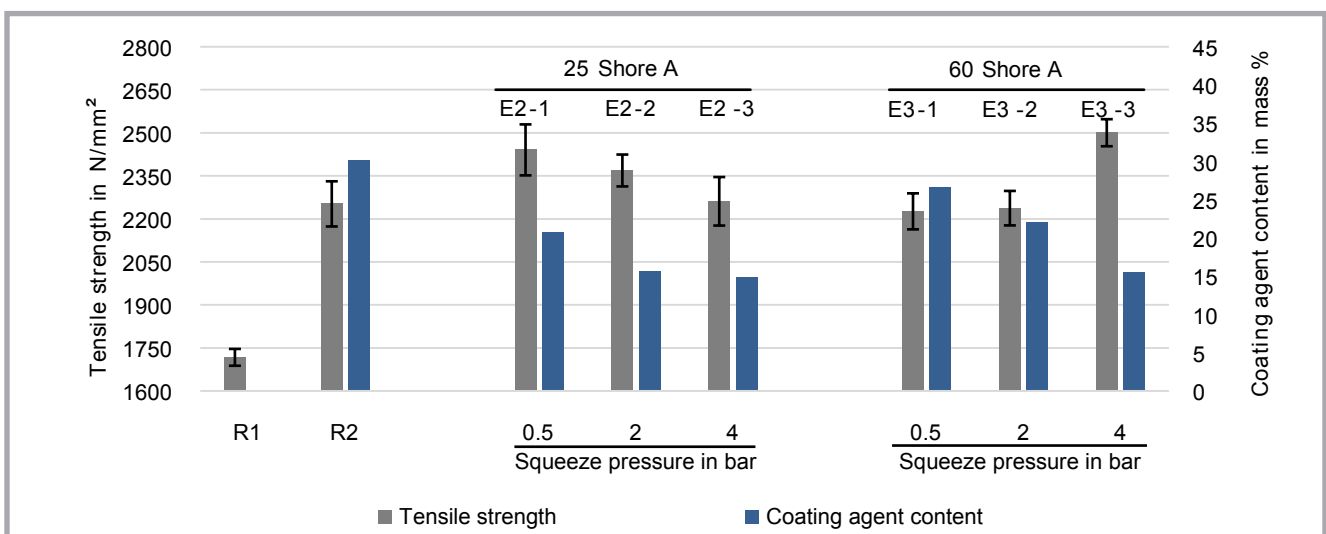


Figure 6. Increasing the squeeze pressure depending on the hardness of the squeeze roll surface (R1: Reference uncoated, R2: Reference coated without squeezing process).

investigations, such as determination of the tensile strength (see **Figure 6**).

E3-3 is squeezed with a high pressure (4 bar) and high hardness of the squeeze roll surface (60 Shore A). As a result, there is a considerable spread of 0° yarns, so that they become elliptical in the area between weft threads. When squeezing with a flexible roll surface (here 25 Shore A), the space for distributing 0° yarns (spread) decreases with increasing pressure, see the schematic in **Table 5**. As a result, the spread of 0° yarns for these samples is lower. The effects on the tensile strength and coating agent content are given in **Figure 6**.

To gain first insights into the coating process supported by ultrasonic vibrations based on CFHT, investigations were made varying the ultrasonic frequency (0 Hz, 25 kHz, and 45 kHz). **Figure 4**

shows the experimental procedure for the ultrasound coating using the example of E5-3.

Findings for the tensile strength and coating agent content as a function of the frequency are given in **Figure 8**.

Evaluation of coating agent content and tensile mechanical characterisation

Results of measurements of the coating agent content and tensile mechanical characterisation are displayed in **Figures 5-8**. As presented in **Table 3**, R1 stands for uncoated CFHT and R2 represents a CFHT coated without the squeeze process.

Figure 5 reveals the relationship between the increasing hardness of the squeeze roll surface (during constant 2 bar squeeze pressure) and both the coating agent con-

tent and tensile strength. The samples of test series E1-1/2 have approximately 5% higher tensile strength than R2. E1-3 shows no significant change in tensile strength compared to R2. The coating agent content increases in comparison to E1-2 (50 Shore A) by about 18%. As the hardness of the squeeze rolls increases, the flexibility of the roll surface is reduced. Therefore with a constant pressure of 2 bar, the squeeze rolls enclose a smaller textile surface with increasing surface hardness, so that more coating material remains on the surfaces of the textile structure. The effect on the tensile strength and coating agent content at higher pressure (up to 4 bar) is shown in **Figure 6**.

The test series E2-1, E2-2 & E2-3 (constant surface hardness of 25 Shore A) suggest that the tensile strength and coating agent content decrease with in-

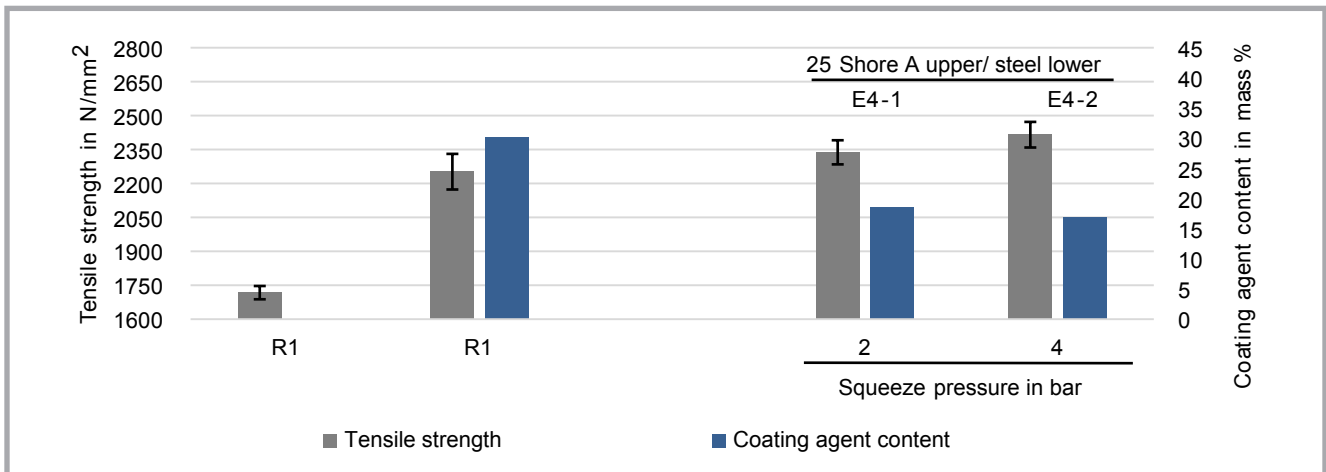


Figure 7. Increasing the squeeze pressure depending on a combination of hardness of squeeze roll surfaces, squeeze roll surface (R1: Reference uncoated, R2: Reference coated without squeezing process).

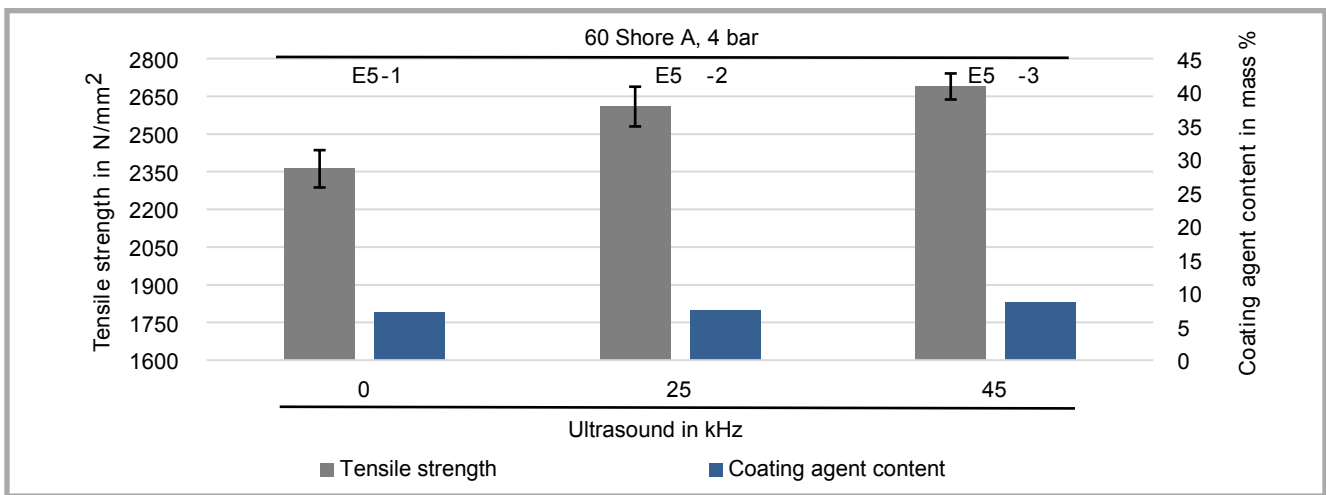


Figure 8. Ultrasonic excitation of the coating agent in E5 the coating agent is subjected to varying frequency (0 kHz, 25 kHz and 45 kHz).

creasing squeeze pressure. Test results of the test series E3-1, E3-2 & E3-3 (constant surface hardness of 60 Shore A) show a different behaviour. Although the coating agent content decreases with increasing squeeze pressure, the tensile strength increases abruptly between E3-2 and E3-3. Between R2 and E3-3, the tensile strength increases by about 10% due to the squeezing process. This distinguishing behavior with respect to tensile strength with increasing pressure between the two types of squeeze roll surface hardness might be caused by the determination exhibited in **Figure 3** and **Table 5**.

Figure 7 represents the results of measurements with squeeze rolls between the upper and lower rolls of different surface hardnesses (lower: steel roll, upper: flexible roll surface with 25 Shore A). Similar to the series of measurements (60 Shore A) in **Figure 5**, an increase in

tensile strength and decrease in coating agent content are recorded. A comparison between E2-3 and E4-2 -both having at least one squeezing roll surface with 25 Shore A – shows that a harder roll surface on one side (steel roll on the lower side) leads to an increase in tensile strength.

In addition to investigations on the squeezing process, initial investigations were carried out on the influence of coating materials excited by ultrasonic waves. The results are provided in **Figure 8**. The basis for the parameters of the squeezing process is the setting of the test series E3-3 (4 bar, 60 Shore A), as these achieve the highest tensile strength.

It was found that the ultrasonic excitation of E5-2 and E5-3 leads to an additional increase in tensile strength of 12% compared to E5-1, due to the better penetration of the coating agent into the roving.

Basically, as the frequency increases, an increase in tensile strength is noted. The coating agent content increases by about 18% between the test series E5-1 to E5-3 due to the better penetration of the coating agent into the roving.

Microsection segment analysis

For microscopic analysis, several consecutive samples were taken from the respective coated grid-like NCF (squeezing process) and single yarns (ultrasonic vibrations). The epoxy resin of the embedding resin has a green colour as it is combined with a fluorescent agent to improve the colour contrast between individual components (see **Table 6**). The black areas represent the individual filaments of CFHT. **Table 6** demonstrates the influence of the squeezing process as well as the ultrasonic vibrations of the roving cross-section structure. According to the analysis of the squeezing process, it is found that squeeze rolls with a

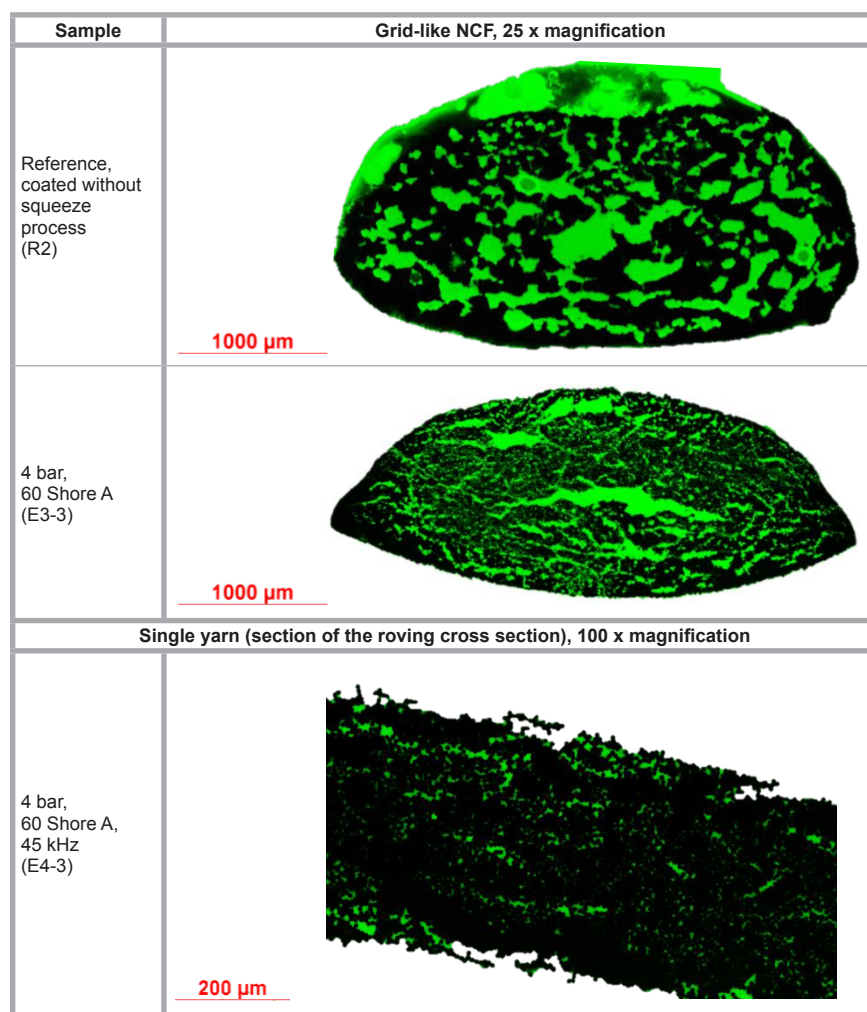
60 Shore A roll surface result in a particular type of fiber spreading. The coating agent distributed around the circumference of the roving, primarily before the squeezing process, and can better penetrate into the core of the roving. However, the filaments within the roving are more evenly distributed, and thus closer to one another; as a result of which the fiber volume content increases. These effects are most evident in the roving cross-section of the E2-6 series, see **Table 6**.

By means of the ultrasound-wave-excited coating agent, the effects described caused by the squeezing process are further enhanced (see **Table 6**, E4-3). The ultrasound waves cause the filaments to slide close together, and air pockets are subsequently reduced.

Conclusions

The results of the research achieved and described in this paper demonstrate that the mechanical strength of grid-like NCF based on CFHT (rovings) can be influenced by the squeezing process, i.e., by regulating the penetration depth of the coating agent. Within this paper, the following squeezing process parameters: 1. squeeze hardness (upper/lower roll surface), 2. squeezing pressure, and 3. the combination of different roll materials between upper/lower rolls were investigated. The test results were evaluated on the basis of measurement of the coating agent content, microsection segment analyses, and tensile mechanical characterisations. The results reveal, inter alia, that an increase in roller pressure (0, 0.5, 2, 4 bar) with a roller hardness of 60 Shore A leads to an increase in tensile strength by up to 10% in comparison to NCF coated without the squeezing process (R2). “Soft” rollers with a hardness of 25 Shore A exhibit no considerably enhanced tensile strength of coated NCF in comparison to R2. In conclusion, it is stated that the highest tensile strength is achieved using 60 Shore A roller hardness and 4 bar squeezing pressure. Also microscopic analyses of the specimens suggest significant differences in the degree of penetration of the rovings with a coating agent between test specimens. It is considered that denser rovings that are more penetrated by the coating agent also have a higher tensile strength compared to samples with a loose arrangement of filaments in the rovings and insufficient impregnation of the coating agent.

Table 6. Example microsection segments of carbon fiber heavy tows (CFHT), R2: without squeeze pressure, only foulard coating; E3-3: 60 Shore A, 4 bar.



In addition, it is shown that if the conventional foulard coating system is supplemented by a module vibrating the coating agent, the strength of the CFHT can be increased even further. This is also achieved by improved penetration of CFHT with a coating agent and increased fiber volume content. The results of this paper form a basis for the design of a suitable coating process. These investigations provide options for significantly improved mechanical performance of CFHT by means of specific squeezing and the use of ultrasonic vibrations during the coating process. Nevertheless further investigations are necessary to ensure the transferability of the findings to other fiber and coating materials.

Acknowledgements

This article presents partial results of the IGF research project 18403 BR/1 of the Forschungsvereinigung Forschungskuratorium Textil e. V. and is funded through the AiF within the program for supporting the

“Industrielle Gemeinschaftsforschung” (IGF) from funds of the Federal Ministry of Economic Affairs and Energy (BMWi) by a resolution of the German Bundestag, such as results of the BMBF project “Carbon Concrete Composites V1.1”.



References

1. Ashir M, Nocke A, Bulavinov A, Pinchuk R, Cherif Ch. Influence of defined amount of voids on the mechanical properties of carbon fiber-reinforced plastics. Polym. Compos. Epub ahead of print 7 March 2018. DOI:10.1002/pc.24820.
2. Ashir M, Hahn L, Kluge A, Nocke A, Cherif Ch. Development of innovative adaptive 3d fiber reinforced plastics based on shape memory alloys. Compos. Sci. Technol. 2016; 126: 43-51.
3. Brameshuber W, Banholzer B, Brümmer G. Ansatz für eine vereinfachte Auswertung von Faser Ausziehversuchen. Beton Stahlbeton. 2000; 95 (12): 702-706.
4. Reinhardt H-W, Krüger M, Grosse C-U. Thin plates prestressed with Textil reinforcement. ACI. 2002; 206: 355-372.

5. Curbach M, Zastrau B. Textilbewehrter Beton-Aspekte aus Theorie und Praxis. Paper presented at: Baustatik-Baupraxis 7 1999. Proceedings of the 7. Fachtagung Baustatik-Baupraxis; 1999 March 18-19; Aachen, DE. Rotterdam: A. A. Balkema 1999, 267-276.
6. Cherif Ch, Diestel O, Engler T, Hufnagl E. In: Textile materials for lightweight constructions. Cherif, Ch.; Springer: Berlin, Heidelberg, New York, Dordrecht, London, 2015; p. 625-646.
7. Kulas C. Zum Tragverhalten getränkter textiler Bewehrungselemente für Betonbauteile. Ph.D. Thesis, Rheinisch-Westfälischen Technischen Hochschule Aachen, Germany; 2013. (German).
8. Shilang X, Krüger M, Reinhardt H-W, Ozbolt J. Bond Characteristics of Carbon, Alkali Resistant Glass, and Aramid Textiles in Mortar. In: J. Mater. Civ. Eng. 2004; 16(4): 356-364.
9. Hahn L, Rittner S, Bauer C, Cherif Ch. Development of alternative bondings for the production of stitch-free non-crimp fabrics made of multiple carbon fiber heavy tows for construction industry. J. Ind. Text. 2018; 48 (3): 660-681.
10. Dolatabadi M K, Janetzko S, Gries T. Geometrical and mechanical properties of a non-crimp fabric applicable for textile reinforced concrete. J. Text. I. 2014; 105 (7), 711-716.
11. Köckritz U. In-Situ Polymerbeschichtung zur Strukturstabilisierung offener näherwirkter Gelege. Ph.D. Thesis, Technische Universität Dresden, Germany, 2007.
12. Krüger M, Reinhardt H-W, Fichtlscherer, M. Bond behaviour of textile reinforcement in reinforced and prestressed concrete. Otto-Graf-Journal 2001; 12: 33-50.
13. Dvorkin D, Peled A. Effect of reinforcement with carbon fabrics impregnated with nanoparticles on the tensile behavior of cement-based composites. Cem. Concr. Res. 2016; 85: 28-38.
14. G Gao S-L, Mäder E, Plonka R. Coatings for glass fibers in a cementitious matrix. Acta Mater. 2004; 52: 4745-4755.
15. Köckritz U, Cherif Ch, Weiland S, Curbach M. In-Situ Polymer Coating of Open Grid Warp Knitted Fabrics for Textile Reinforced Concrete Application. J. Ind. Text. 2010; 40 (2): 157-169.
16. Younes A, Seidel A, Rittner S, Cherif Ch, Thyroff R. Innovative textile Bewehrungen für hochbelastbare Betonbauteile. Beton- und Stahlbetonbau 2015; 110: 16-21.
17. Lorenz E, Ortlepp R. Bond Behavior of Textile Reinforcements – Development of a Pull-Out Test and Modeling of the Respective Bond versus Slip Relation. J. Mater. Civ. Eng. 2012; 6: 479-486.
18. DIN EN 12127 (1997). DIN Deutsches Institut für Normung.
19. ISO 3341:2000-05. 2000-05 (2000). International Organization for Standardization.

☐ Received 30.04.2018 Reviewed 09.07.2018

The Scientific Department of Unconventional Technologies and Textiles specialises in interdisciplinary research on innovative techniques, functional textiles and textile composites including nanotechnologies and surface modification.

Research are performed on modern apparatus, *inter alia*:

- Scanning electron microscope VEGA 3 LMU, Tescan with EDS INCA X-ray microanalyser, Oxford
- Raman InVia Reflex spectrometer, Renishaw
- Vertex 70 FTIR spectrometer with Hyperion 2000 microscope, Brüker
- Differential scanning calorimeter DSC 204 F1 Phenix, Netzsch
- Thermogravimetric analyser TG 209 F1 Libra, Netzsch with FT-IR gas cuvette
- Sigma 701 tensiometer, KSV
- Automatic drop shape analyser DSA 100, Krüss
- PGX goniometer, Fibro Systems
- Particle size analyser Zetasizer Nano ZS, Malvern
- Labcoater LTE-S, Werner Mathis
- Corona discharge activator, Metalchem
- Ultrasonic homogenizer UP 200 st, Hielscher

The equipment was purchased under key project - POIG.01.03.01-00-004/08 Functional nano- and micro textile materials - NANOMITEX, co-financed by the European Union under the European Regional Development Fund and the National Centre for Research and Development, and Project WND-RPLD 03.01.00-001/09 co-financed by the European Union under the European Regional Development Fund and the Ministry of Culture and National Heritage.



Textile Research Institute
Scientific Department of Unconventional Technologies and Textiles
Tel. (+48 42) 25 34 405
e-mail: cieslakm@iw.lodz.pl